Efficient photocatalytic partial oxidation of aromatic alcohols by using ZnIn$_2$S$_4$ under green conditions

Muhammad Umair, Claudio Maria Pecoraro, Francesco Di Franco, Monica Santamaria, Leonardo Palmisano, Vittorio Loddo, Marianna Bellardita[*]

Engineering Department, University of Palermo, Viale delle Scienze Ed. 6, Palermo 90128, Italy.

Corresponding author: Prof. Marianna Bellardita. E-mail address: marianna.bellardita@unipa.it

Abstract

The ternary chalcogenide ZnIn$_2$S$_4$ (ZIS) has been synthesized by a simple hydrothermal method in which the carcinogen thiacetamide, universally used as a precursor, has been, for the first time, replaced successfully with the harmless thiourea. ZIS has been used as photocatalyst for the partial oxidation of different aromatic alcohols to their corresponding aldehyde in water solution, under ambient conditions and simulated solar light irradiation. The photocatalytic performances of ZnIn$_2$S$_4$ were better than TiO$_2$ P25. In the presence of ZIS for 4-methoxybenzyl alcohol, piperonyl alcohol, and benzyl alcohol, a selectivity towards the corresponding aldehyde of 99% for a conversion of 46%, 75% for a conversion of 81%, and 87% for a conversion of 25%, respectively, was obtained. For the same alcohols a selectivity of 19% for a conversion of 41%, 19% for a conversion of 13%, and 16% for a conversion of 26%, was observed in the presence of TiO$_2$ P25.

Keywords: Photocatalysis; ZnIn$_2$S$_4$; Aromatic alcohols partial oxidation; Solar light; Aqueous medium.

1. Introduction

Heterogeneous photocatalysis has established itself as a green process based on light-activated semiconductor materials for H$_2$ production, wastewater treatment, CO$_2$ reduction and the conversion of organic substances into valuable chemicals, thanks to its sustainability, low environmental impact and the possibility of using natural sunlight [1–10]. This technology has not

been widely applied on an industrial scale due to some weaknesses regarding, for example, costs and efficiency. However, photocatalytic processes can be performed using economical and environmentally friendly semiconductors under low temperature and pressure, in the presence of atmospheric O_2 as a non-toxic oxidizing agent and water as a solvent. Furthermore, if appropriate materials are used, sunlight can be used as an irradiation source.

For these reasons, the photocatalytic approach, in addition to being scientifically intriguing due to its interdisciplinarity, should be considered very carefully for its versatility even just for niche applications. In fact, traditional technologies typically require more severe operating conditions such as the use of harmful oxidizing agents and generally organic solvents.

Nevertheless, it should be noted that some drawbacks of photocatalysis, such as the activation of catalysts by irradiation with UV light, the low selectivity towards partial oxidation products (especially when water is used as the solvent) and the challenge of working with highly concentrated solutions have not yet been fully resolved [9,11,12]. However, basic laboratory-scale studies are necessary to verify the feasibility and effectiveness of the process especially when new photocatalysts are used.

Although among different semiconductors TiO_2 has played an important role in the selective oxidation of aromatic alcohols [13–17], increasing attention is currently paid to the search for alternative photocatalysts with greater absorption of sunlight and better efficiency towards partial oxidation reactions in aqueous medium [18–21].

In particular, the selective photocatalytic oxidation of aromatic alcohols to the corresponding aldehydes has led to numerous applications in the pharmaceutical and food industries [9,10,22–24], but a significant progress is still needed. For the selective oxidation of some alcohols to the corresponding aldehydes, narrow-band semiconductor materials, e.g. CdS [25], In_2S_3 [26], g-C_3N_4 [27,28], have shown higher photocatalytic activity than TiO_2.

Among several alternative catalysts to TiO_2, metal chalcogenides have attracted attention in recent years for their remarkable catalytic properties, chemical stability, and narrow band gap in different fields. Zinc indium sulfide, ZnI_2S_4, a ternary metal chalcogenide belonging to the AB_2X_4 ternary compound family, represents a high potential photocatalyst thanks to its low toxicity, its narrow band-gap (2.06-2.85) eV which allows the use of visible light and its chemical stability [29–33]. Moreover, energy values of the valence and conduction bands are suitable for the oxidation of organic compounds and the reduction of H^+, respectively [30,32,34–37]. For these reasons, recently

ZnI$_2$S$_4$ has been employed for some photocatalytic reactions such production of H$_2$ [30,38], [37], removal of organic pollutants [39] and selective conversion of some alcohols, often carried out in the presence of organic solvents [40,41]. The material exists in three crystalline phases, i.e. the cubic, the hexagonal and the rhombohedral and can have different morphological characteristics (nano/micro particles, nanotubes, microspheres) depending on the conditions under which it is synthesized. The photocatalytic activity strongly depends on the type of polymorph chosen and its morphology [39,42–45].

In this paper, ZnIn$_2$S$_4$ was synthesized via the hydrothermal route using indium chloride, zinc chloride and thiourea in ethanol as the solvent. Thiourea has been used as a replacement for the carcinogenic thioacetamide, which has been used extensively in the past [34,38,40,41,45,46].

Structural, surface and electrochemical techniques allowed to characterize the powdered ZnIn$_2$S$_4$ photocatalyst which was used in selective oxidation of different aromatic alcohols i.e., benzyl alcohol (BA), furfuryl alcohol (FA), piperonyl alcohol (PA), cinnamyl alcohol (CA), vanillyl alcohol (VA), 4-methoxybenzyl alcohol (4MBA), 4-nitrobenzyl alcohol (4NBA), 4-hydroxybenzyl alcohol (4HBA), and 2-hydroxybenzyl alcohol (2HBA) in water solution under simulated solar light irradiation. The photoactivity was compared with that of the widely used Aeroxide TiO$_2$ P25, one of the most studied photocatalyst.

2. Experimental section

Chemicals

Indium chloride (≥99.99% Labfor), zinc chloride (≥98+% Sigma-Aldrich), thiourea (≥99% Sigma-Aldrich), benzyl alcohol (>98% Aldrich), benzaldehyde (98% Sigma-Aldrich), benzoic acid (98% Sigma-Aldrich),

4-nitrobenzyl alcohol (>98% Aldrich), 4-nitrobenzaldehyde (98% Sigma-Aldrich), 4-nitrobenzoic acid (>98% Aldrich), 4-methoxybenzyl alcohol (Fluka 98%), 4-methoxybenzaldehyde (98% Sigma-Aldrich), 4-methoxybenzoic acid (98% Sigma-Aldrich), 2-hydroxybenzyl alcohol (>98% Aldrich), 2-hydroxybenzyl aldehyde (99.8% Aldrich), 2-hydroxybenzoic acid (98% Sigma-Aldrich), 4-hydroxybenzyl alcohol (>98% Aldrich), 4-hydroxybenzyl aldehyde (99.8% Aldrich), 4-hydroxybenzoic acid (98% Sigma-Aldrich), furfuryl alcohol (98% Sigma-Aldrich), furfural

(98% Sigma-Aldrich), 2-furoic acid (98% Sigma-Aldrich), piperonyl alcohol (>98% Aldrich), piperonal (99% Sigma-Aldrich), piperonylic acid (98% Sigma-Aldrich), cinnamyl alcohol (98% Sigma-Aldrich), cinnamic aldehyde (98% Sigma-Aldrich), cinnamic acid (98% Sigma-Aldrich), vanillyl alcohol (98% Sigma-Aldrich), vanillin (98% Sigma-Aldrich), vanillic acid (98% Sigma-Aldrich), Aeroxide TiO_2 P25 and ethanol were used without further purification.

Catalyst preparation

Thiourea was used to the best of our knowledge for the first time as a sulfur precursor to synthesize $ZnIn_2S_4$ instead of carcinogenic thioacetamide.

Typically, 261.12 mg of $ZnCl_2$, 848.64 mg of $InCl_3$, and 584.56 mg of thiourea were dissolved in 200 ml absolute ethanol. The mixture was stirred for 30 minutes until the formation of a clear solution and then it was heated at 80 ºC for 2h. Subsequently, the resulting solution was transferred to a stainless-steel autoclave and heated at 180 ºC for 18h. After that, the autoclave was cooled down to ambient temperature and the resulted solid was recovered. The synthetic route of the preparation of $ZnIn_2S_4$ (ZIS) powder is shown in Figure 1.
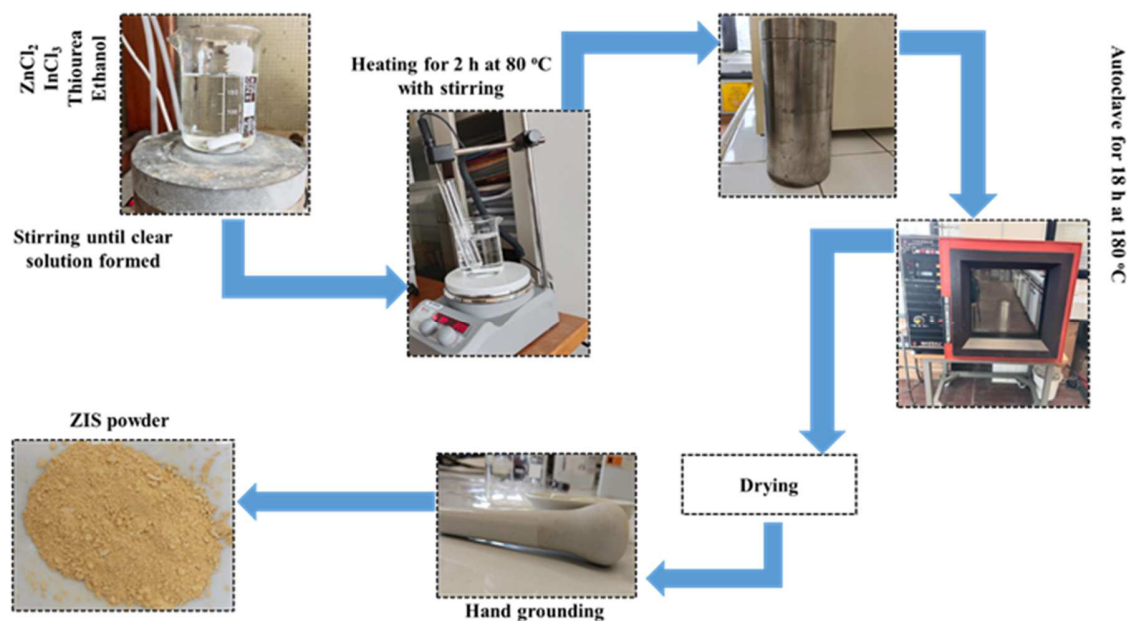
Figure 1. Synthetic route of ZIS powder.

Characterizations

UV-Vis diffuse reflectance spectra (DRS) were recorded at room temperature by means of a Shimadzu UV-2401 PC spectrophotometer using $BaSO_4$ as the reference material. The value of the optical band-gap was obtained by plotting the modified Kubelka-Munk function, $[F(R'_\infty)h\nu]^{1/2}$ versus the energy of the exciting light.

The specific surface area (SSA) was measured by a Flow Sorb 2300 Micromeritics apparatus using the single-point BET method.

The sample morphology was investigated by scanning electron microscopy (SEM) using a FEI Quanta 200 ESEM microscope operated at an accelerating voltage of 30 kV. X-ray diffraction (XRD) pattern of the prepared sample was recorded by a Philips diffractometer using the CuK_α radiation under a current of 30 mA and a voltage of 40 kV. The 2θ investigated scan range was set from 20 to 60° with a scan rate of 3°/min.

Photoelectrochemical measurements were carried out using a three-electrode configuration cell in a 0.1 M aqueous solution of ammonium pentaborate (ABE) at a pH of approximately 9. The ZIS photocatalyst was immersed in the ABE solution after drop-casting onto a carbon paper support (Toray 40% wet Proofed-E-Tek). A platinum wire served as the counter electrode, while a silver/silver chloride (Ag/AgCl/sat. KCl) electrode was used as the reference electrode (0 V vs Ag/AgCl = 0.197 V vs SHE). Photocurrent spectra were obtained by irradiating the samples through the quartz window of the cell using a 450 W UV-VIS xenon lamp and a monochromator, with the wavelength varied at a fixed potential. Electrode potential was controlled using a potentiostat, and the signal corresponding to the measured current was sent to a two-phase lock-in amplifier to isolate the photocurrent from the overall cell current. To interrupt the irradiation at a known frequency (specifically, 13 Hz), a mechanical chopper was employed. The flat bland potential was determined by plotting the photocurrent versus the applied potential at a fixed wavelength.

Photocatalytic activity

Photocatalytic activity runs were carried out in a Pyrex photoreactor (internal diameter: 52 mm, external diameter: 56 mm and height 200 mm) containing 150 mL of the aqueous suspensions. All the runs were performed in the open air, at room temperature and under the natural pH of each of the alcohols used in the presence of the catalyst. The initial concentration of all the substrates was 0.5 mM. The irradiation source, a 50 W halogen lamp, was placed axially at the center of the

reactor. Water was circulated through the Pyrex thimble of a cooling jacket to maintain the temperature at approx. 30°C. The quantity of catalyst was determined by photon absorption determinations through transmittance measurements with a Delta Ohm DO9721 radiometer placed on the external wall of the photoreactor, choosing the quantity (1 g/L) for which almost 90% of the photons emitted by the lamp were absorbed by the photocatalyst, and consequently the transmitted light measured by the radiometer was ca. 10%. After measuring the initial concentration of the substrate, the catalyst was added and stirred in the dark for 30 minutes to reach the adsorption-desorption equilibrium, then the lamp was switched on. Samples were withdrawn after each hour and filtered through 0.25 µm membrane (HA Millipore) to remove the solid particles. A Beckman coulter HPLC apparatus supplied with a Diode Array detector was used to identify and to calculate the concentrations of the substrates and of the produced intermediates. A Phenomenex KINETEK 5 µm C18 column was used, and the eluent (flow 0.8 mL min^{-1}) consisted of a mixture of acetonitrile and 13 mM trifluoroacetic acid (20:80 v:v). Standards of alcohols and their intermediates were used to identify the products and to obtain the calibration curves.

For some peculiar aldehydes, i.e. 2-hydroxybelzaldehyde, 4-hydroxybelzaldehyde, furfuryl aldehyde and vanillin, adsorption tests in the dark were done to value the interaction of the substrates with the catalyst surface. 1 g of ZIS was added to 100 mL of aldehydes 0.5 mM aqueous solution and the dispersions were left in the dark under stirring for 2 hours, and after this time the concentration of the substrate still present in solution after reaching the adsorption-desorption equilibrium was measured.

In order to investigate the role of the main active species generated under irradiation in the photocatalytic system, runs in the presence of selected scavengers (1mM) were done in the presence of piperonyl alcohol. Namely, tert-butanol was used as $^{\bullet}$OH scavenger, AgNO$_3$ as electrons scavenger, Na$_2$C$_2$O$_4$ as holes scavenger and 1,4-benzoquinone BQ as a $^{\bullet}$O$_2{}^{-}$ scavenger [47–49].

3. Results and Discussion

The UV-vis diffuse reflectance spectrum of the ZnIn$_2$S$_4$ photocatalyst is reported in Figure 2. The spectrum indicates the occurrence of a significant light absorption in the visible range with a steep absorption edge between 420 and 500 nm corresponding to the band-to-band transition of the

material [50]. The optical band gap of $ZnIn_2S_4$ is 2.58 eV and was calculated considering the powder as an indirect semiconductor by plotting the modified Kubelka-Munk function, $[F(R`\infty)h\nu]^{1/2}$, versus the energy of the exciting light (inset of Figure 2).
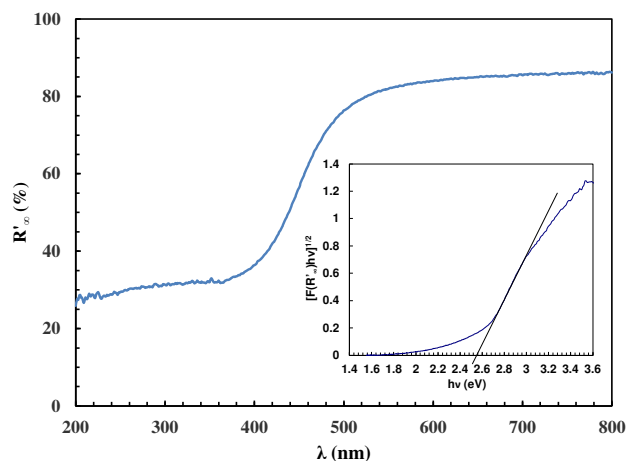

Figure 2. UV-vis diffuse reflectance spectra of $ZnIn_2S_4$ photocatalyst. Inset: Tauc plot for band-gap determination.

Figure 3 presents the XRD pattern of the $ZnIn_2S_4$ sample. All the diffraction peaks are consistent with the hexagonal phase of $ZnIn_2S_4$ (JCPDS No. 65-2023) [40]. The BET surface area of the powders resulted to be 1 m^2 g^{-1}.
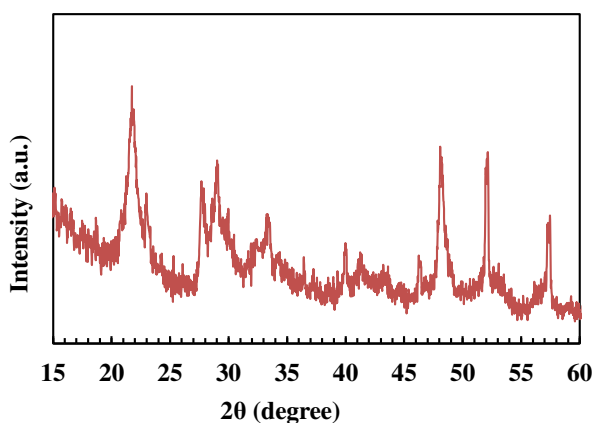
Figure 3. XRD pattern of the sample $ZnIn_2S_4$.

The SEM images of the sample (Figure 4 a,b,c) show the formation of numerous flower-shaped microspheres with a diameter between 3 and 6 μm similarly to what is reported in the literature for ZIS prepared from thioacetamide. An enlargement of the surface highlights the formation of several flaked layers. EDS mapping demonstrates the presence of Zn, In and S and their uniform distribution. The atomic percentage of the elements was found to be 8%, 23% and 36% for Zn, In and S, respectively, in good accordance with the ZIS molecular composition.
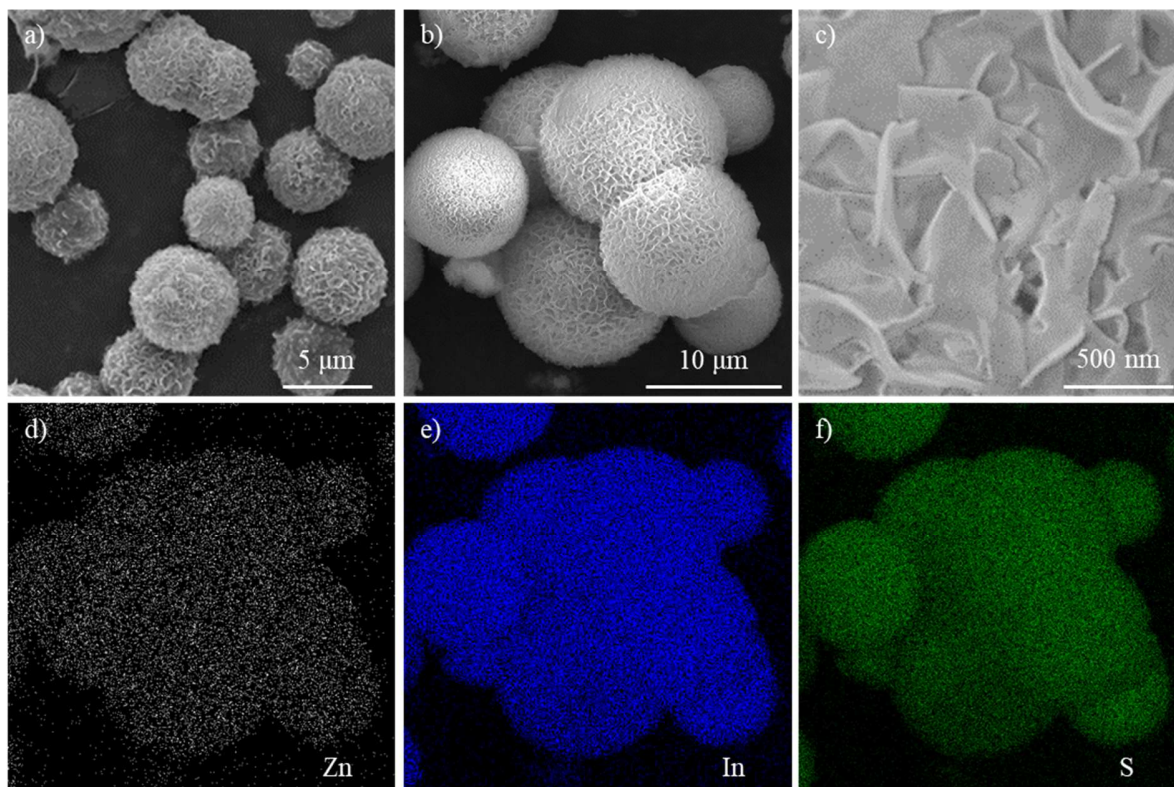

Figure 4. SEM images of the sample $ZnIn_2S_4$ at different magnifications (a,b,c), and EDS mapping images related to Zn (d), In (e) and S (f).

Electrochemical characterizations were performed to obtain more information on the intrinsic electronic properties of the photocatalyst. Figure 5a illustrates the photocurrent spectrum, recorded in a 0.1 M ABE solution by polarizing the ZIS supported on carbon paper (see experimental section) at the open-circuit potential measured in this electrolyte (i.e. 0.35 V versus Ag/AgCl). To estimate the optical band gap (E_g) of the material, the following equation was employed:

$$(Q_{ph} \cdot h\nu)^n \propto h\nu - E_g$$

where hv represents the energy of the photon, n = 0.5 because the occurrence of a non-direct optical transition is assumed, and Q_{ph} is the photocurrent yield [51,52]. The latter is the measured photocurrent adjusted for lamp efficiency and it is proportional to the light absorption coefficient at photon energy close to that of the band gap. As depicted in Figure 5b, the optical band gap was estimated by extrapolating the $(Q_{ph} \cdot hv)^{0.5}$ vs hv plot to zero. $E_g \sim 2.7$ eV was estimated, in agreement with the other results reported in the literature [53] and with the experimental results obtained from diffuse reflectance spectroscopy (DRS). In order to estimate the flat band potential of ZIS, the dependence of I_{ph} on potential was studied under constant irradiating wavelength (see Figure 5c). The photocurrent decreases as soon as the potential decreases, as expected for n-type semiconducting material, and $I_{ph} = 0$ at ~ 0.25 V vs Ag/AgCl, thus suggesting a flat band potential (E_{fb}) around this value.
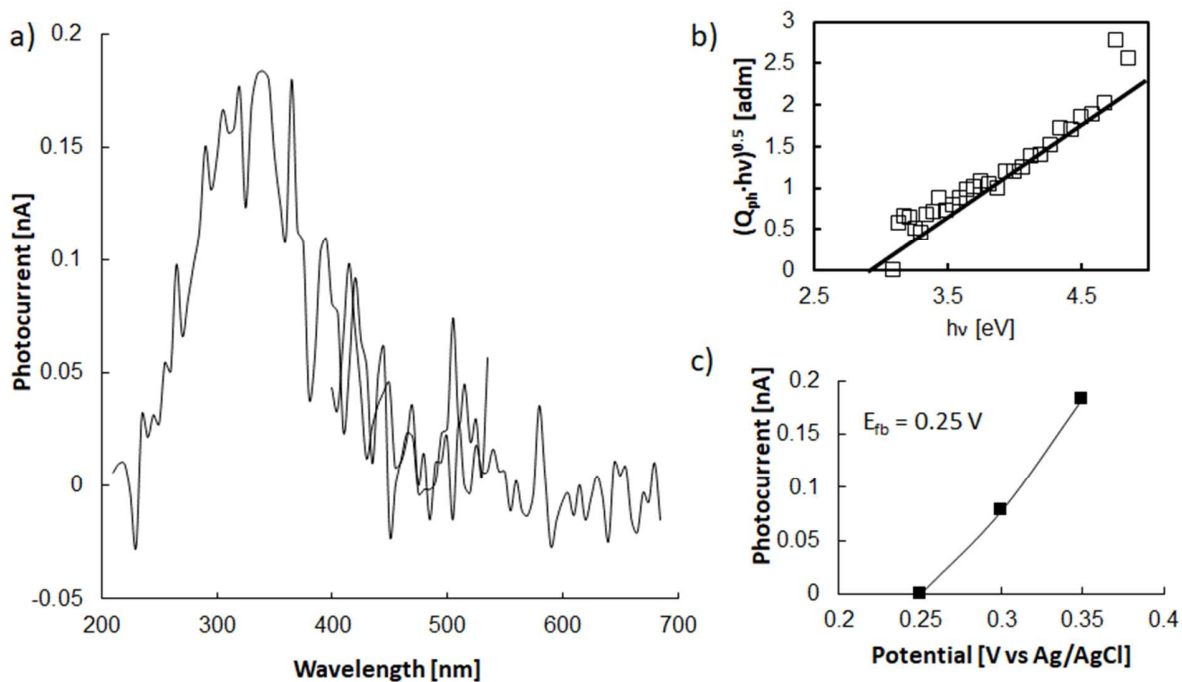
Figure 5. a) Photocurrent spectra of $ZnIn_2S_4$ recorded in 0.1 M ABE and Open Circuit Potential of 0.35 V vs Ag/AgCl. The respective $(Q_{ph} \cdot hv)^{0.5}$ vs hv is shown in b). Photocurrent vs potential recorded at 345 nm is reported in c).

Photoreactivity results

The results of the photoactivity runs with different substrates i.e., benzyl alcohol (BA), furfuryl alcohol (FA), piperonyl alcohol (PA), cinnamyl alcohol (CA), vanillyl alcohol (VA), 4-methoxybenzyl alcohol (4MBA), 4-nitrobenzyl alcohol (4NBA), 4-hydroxybenzyl alcohol (4HBA), and 2-hydroxybenzyl alcohol (2HBA) are reported in Figure 6, in which the evolution of the concentrations of the different alcohols and corresponding aldehydes and acids are plotted versus irradiation time.

For the various alcohols a different amount of converted substrate and formed intermediates can be observed, confirming the finding that for each catalyst an absolute photocatalytic activity must not be considered but it must always be contextualized to the individual substrate [23,42]. It should be taken into account, of course, the specific interactions between the photocatalyst and the organic compounds (both the chemical structure of the aromatic alcohols and of the formed compounds) [23,54–56].

Figure 6. Evolution of the concentration vs. time for different alcohols with ZIS (Alcohol ○, aldehyde □ and acid △) under simulated solar light irradiation.

In Table 1 are reported the values of alcohols conversion (X), selectivity (S) and yield (Y) towards the main intermediates, after 5h of irradiation. The following equations were used for the determination of X, S and Y:

$$X = \frac{[Alcohol]i - [Alcohol]t}{[Alcohol]i} * 100$$

$$S = \frac{[P]t}{[Alcohol]i - [Alcohol]t} * 100$$

$$Y = \frac{[P]t}{[Alcohol]i} * 100$$

where: [Alcohol]i and [Alcohol]t indicate the initial molar concentration and molar concentration at time t of the different alcohols, respectively. [P]t is the molar concentration of the obtained product (aldehyde or acid) at time t.

It is worth mentioning that ZIS photocatalyst was active under solar light irradiation for the selective partial oxidation of all the used alcohols and the obtained products were principally aldehydes and trace amounts of acids.

After 5h of irradiation, the conversion degree ranges between 13 and 81% being the lowest figures obtained with FA and the two OH-substituted benzyl alcohols (4HBA and 2HBA) and the highest one with PA. High selectivity values were obtained with almost all the substrates except for 4NBA, CA and VA.

Previous literature data in the presence of TiO_2 based photocatalysts have shown that selectivity is high when the conversion is low, and its increase corresponds to a decrease in selectivity [57]. By using ZIS photocatalyst high values of both conversion and selectivity were achieved for many substrates. These results appear very satisfactory considering that the reactions have been carried out in pure water and under simulated solar light irradiation, contrary to what is often reported in

the literature [41]. Under these conditions the photocatalysts performance is generally lower than in the presence of organic co-solvents and UV light irradiation [28,58]. Furthermore, it must also be considered that when using organic solvents, the runs are carried out with small reaction volumes (1.5 mL) and a high catalyst amount (5.3 g L^{-1}) [41,59].

For BA, after 5h of irradiation the conversion was 25% while the selectivity reached 87%. An electron donating substituent group as -O-CH$_3$ in *para* position (4MBA) induced higher conversion (46%), and selectivity (99%), in accordance with literature [60]. In fact, being an ortho-para orienting group, the methoxy group in the para position favors the attack on the benzyl group in the para position by the oxidizing species in the conversion of alcohol into aldehyde [28]. Furthermore, the inductive and delocalization effects hinder a subsequent oxidizing action towards the aromatic ring, avoiding its significant mineralization and therefore essentially favoring the partial oxidation reaction. Notably, by using ZIS as photocatalyst both conversion and selectivity were improved with respect TiO$_2$ based samples [13,60]. By starting from 4NBA the conversion was 27% and the selectivity 11%. In accordance with Yurdakal et al. [61] the presence of –NO$_2$ group in the *para*-position of the aromatic ring, being an electron withdrawing group, had a detrimental effect on the selectivity while the conversion was substantially the same to that of BA.

For the 4HBA and 2HBA substrates the ZIS photocatalyst showed the same low conversion (only 13%) while the selectivity towards the corresponding aldehyde starting from 4HBA was higher than that which occurred in the presence of 2HBA, confirming that the selectivity is greater when the substituent is in the meta position compared to the ortho position [62]. As was previously demonstrated using TiO$_2$ photocatalysts [54], this result can be attributed to the lower adsorption of 4-hydroxybelzaldehyde compared to 2-hydroxybelzaldehyde also on the surface of the ZIS photocatalyst. Adsorption tests in the dark of the two aldehydes confirmed this hypothesis being negligible the amount 4-hydroxybelzaldehyde adsorbed onto ZIS surface after 2h of stirring and 65% the percentage of adsorbed 2-hydroxybelzaldehyde. By increasing the irradiation time up to 7h a higher conversion and a lower selectivity has been noticed.

For FA a low degree of both conversion and selectivity was obtained contrary to what was observed using UV light with TiO$_2$ photocatalysts for which high selectivity values were obtained at low conversion values [3]. The percentage of adsorbed furfuryl aldehyde after 2h adsorption on the dark was 35%, and this data can justify the low selectivity. Irradiation for longer times (7.5h instead of 5h) showed a conversion increase up to 36% with the same selectivity value.

ZIS showed a high activity towards the partial oxidation of PA (conversion 81%) to piperonal (selectivity 75%) being the yield after 5 hours of 60%, while starting from CA a high conversion and low selectivity was noted. For VA the conversion and selectivity were 36% and 10%, respectively with a low degree of adsorption of the aldehyde (8%) on the catalyst surface. The results reached in the presence of PA are very satisfactory by considering the results obtained with TiO_2 and C_3N_4 photocatalysts under both UV and simulated solar light irradiation [28,63].

Table 1. Conversion (X) of different alcohols, selectivity (S) and yield values towards the corresponding aldehydes and acids after 5h of irradiation by using the home prepared $ZnIn_2S_4$. In the green boxes, runs conducted for more than 5 hours.

Substrates	X	S_{Ald}	S_{Acid}	Y_{Ald}	Y_{Acid}
BA	25	87	14	21	5
4MBA	46	99	negligible	47	negligible
4NBA	27	11	9	3	2
4HBA	13	93	3	12	negligible
4HBA	28 (7h)	14	1.5	4	negligible
2HBA	13	60	7	8	1
2HBA	28 (7.5h)	9	negligible	2	negligible
FA	13	32	0	15	0
FA	36 (7.5h)	31	negligible	11	negligible
PA	81	75	6	60	5
CA	73	15	0	11	0
VA	36	10	19	4	7

Overall, the results obtained using ZIS for the selective synthesis of valuable chemicals such as aldehydes under green conditions are encouraging. In fact, in many cases high selectivity values combined with high conversions have been obtained.

In Table 2 are reported the conversion and selectivity values related to the different alcohols obtained with the commercial widely used TiO_2 P25 in the same experimental conditions of ZIS. For the sake of comparison, for the different alcohols are considered similar conversion degrees as those reported in Table 2 and the corresponding irradiation times, t, necessary to reach that conversion degree. As can be seen, with the exception of 4NBA, higher selectivity values at the

same alcohols conversion degree were always obtained with ZIS. The results showed in Table 2 confirm that TiO_2 generally have a higher oxidant power than ZIS (Table 1), being the same conversion reached in less time and the selectivity values lower.

Table 2. Conversion (X) of different alcohols, time (t) necessary to reach the reported conversion, selectivity (S) and yield values (Y) towards the corresponding aldehydes and acids in the presence of commercial TiO_2 P25.

| Substrates	X	t	S_{Ald}	S_{Acid}	Y_{Ald}
BA	26	2.5h	16	7	4.3
4MBA	41	4h	19	-	7.0
4NBA	22	4h	18	11	4.0
4HBA	13	4h	10	-	1.8
2HBA	13	5h	23	-	3.0
FA	13	1.5h	13	1	1.5
PA	13	3h	19	-	2.5
CA	65	8h	8	-	5.8
VA	35	5h	9	35	3.3

Figure 7a shows the degradation of piperonyl alcohol under irradiation in the presence of ZIS and various scavengers. The results indicate that the main active species in PA degradation are e^- since the lowest photoactivity is observed after the addition of $AgNO_3$. Also in the presence of benzoquinone a significant reduction in photoactivity is noted which highlights the important role of $^\bullet O_2^-$ radicals. These results are in agreement with each other considering that under irradiation the $^\bullet O_2^-$ radicals are formed from the reaction between O_2 and the photogenerated e^-. The presence of $AgNO_3$ reduces the amount of e^- available, and therefore decreases the production of $^\bullet O_2^-$. A less pronounced decrease in activity can be noted in the presence of $Na_2C_2O_4$ and tert-butanol indicating a minor role of holes and hydroxyl radicals.
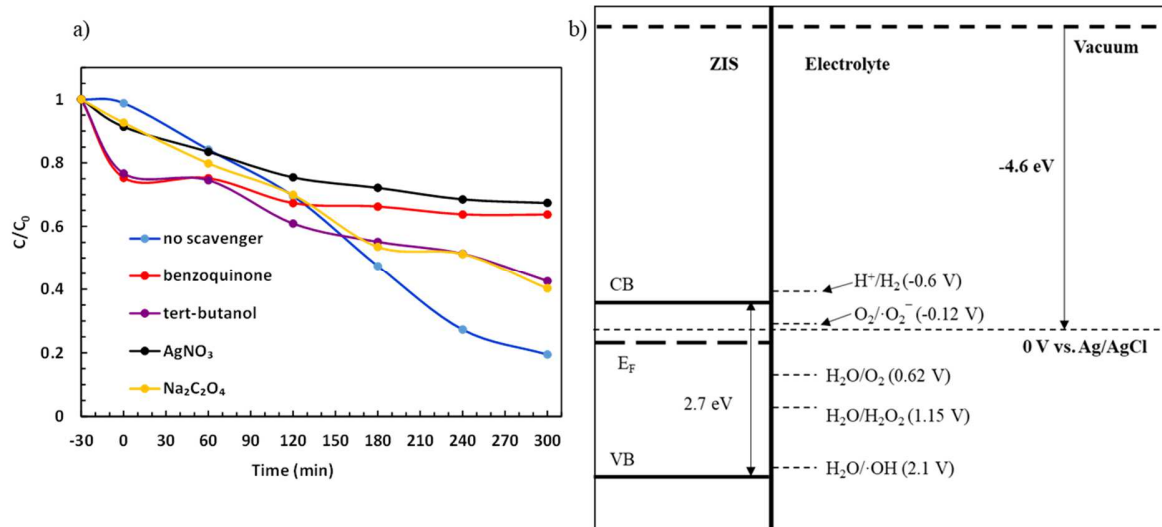
Figure 7. a) Photocatalytic degradation of PA with ZIS in the presence of different scavengers and b) energetic sketch of the semiconductor/electrolyte interface.

These experimental findings can be also supported by the energetics of the ZIS/electrolyte interface reported in Figure 7b, drawn taking into account the electrochemical measurements. The VB edge of the material is located at -6.85 eV in agreement with the results reported in ref. [64], thus allowing to locate the CB edge at $\sim$ -4.1 eV (the optical band gap being $\sim$ 2.7 eV). The band edge energy location is consistent with the estimated flat band potential (see Figure 6b) and with the reactivity of the photocatalyst under irradiation. Indeed, the generated holes are noble enough to produce hydroxyl radicals, while the photogenerated electrons can induce oxygen reduction to produce $^{\bullet}O_2^{-}$. It is also worth mentioning that the conduction band edge energy location suggests that hydrogen evolution is not thermodynamically possible. This statement is supported experimentally by gas chromatographic analyses, carried out during partial oxidation of FA, since hydrogen is not revealed up to 5 h of irradiation.

In Figure 8 is proposed a reaction scheme drawn in accordance with the above reported results. The photoexcited electrons and holes migrate towards the ZIS surface. These results agree with each other because the electrons react with molecular oxygen to form the superoxide radical ($^{\bullet}O_2^{-}$) and these, together with holes, attack the aromatic alcohols transforming them into the corresponding aldehydes.
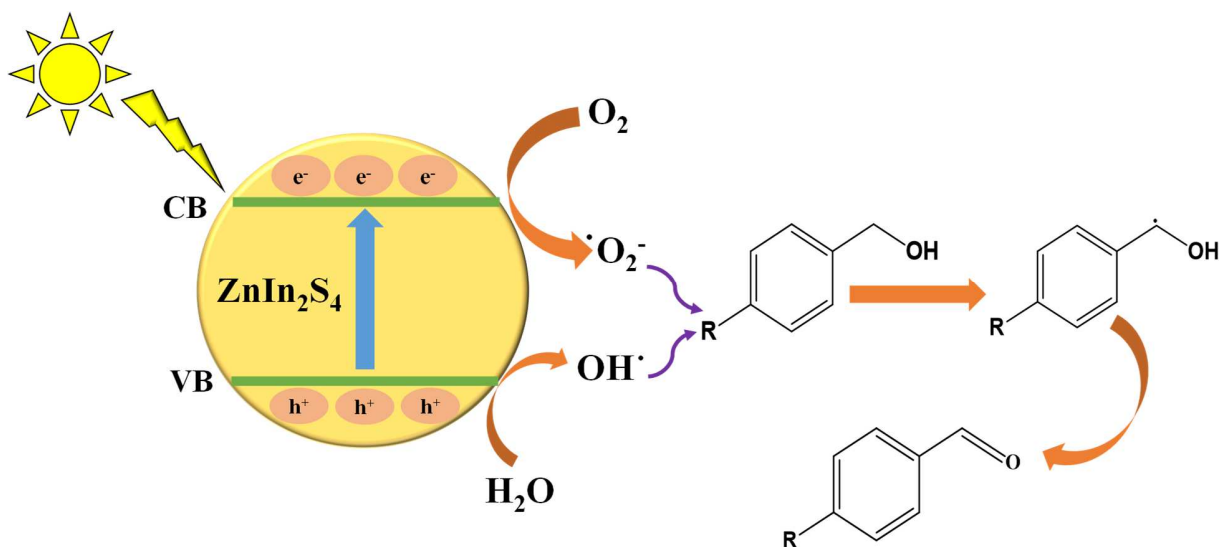
Figure 8. Hypothesized reaction pathway.

Conclusions

ZnIn$_2$S$_4$ photocatalyst synthesized by a facile hydrothermal method exhibited high photoactivity for the selective partial oxidation of different aromatic alcohols to their corresponding valuable aldehydes under green conditions. The performance of ZIS was higher than that of the benchmark TiO$_2$ P25 highlighting the use of this new catalyst as a very effective substitute for TiO$_2$ in selective syntheses under sunlight irradiation and aqueous medium. Furthermore, in this case one of the disadvantages of synthetic photocatalysis is also overcome, namely the low conversion of the substrate to obtain high selectivity. In fact, it has been seen that for many alcohols it has been possible to obtain high selectivity values with good degrees of conversion of the different substrates. Therefore, this can be considered a preliminary fundamental study, precisely to verify the efficiency of the process. A subsequent development could include the coupling with an aldehyde separation system, for example the use of selective membranes, which allow maximizing both conversion and yield, even if it is not easy to select a suitable membrane both from the engineering and chemical point of view for molecules that are too similar.

References

[1] R. Singh, S. Dutta, *Fuel* **2018**, *220*, 607–620.

[2] R. Fiorenza, S. Sciré, L. D'Urso, G. Compagnini, M. Bellardita, L. Palmisano, *Int J Hydrogen Energy* **2019**, *44*, 14796–14807.

[3] C. M. Pecoraro, M. Bellardita, V. Loddo, D. Virtù, F. Di Franco, M. Santamaria, *Appl Catal A Gen* **2023**, *650*, DOI 10.1016/j.apcata.2022.118987.

[4] A. Shokri, M. Sanavi Fard, *Chemical Papers* **2022**, *76*, 5309–5339.

[5] M. Umair, T. Kanwal, V. Loddo, L. Palmisano, M. Bellardita, *Catalysts* **2023**, *13*, 1440.

[6] M. Bellardita, A. Di Paola, E. García-López, V. Loddo, G. Marcì, L. Palmisano, *Send Orders for Reprints to Reprints@benthamscience.Net Photocatalytic CO 2 Reduction in Gas-Solid Regime in the Presence of Bare, SiO 2 Supported or Cu-Loaded TiO 2 Samples*, **2013**.

[7] R. Camarillo, S. Tostón, F. Martínez, C. Jiménez, J. Rincón, *J Supercrit Fluids* **2017**, *123*, 18–27.

[8] F. Parrino, M. Bellardita, E. I. García-López, G. Marcì, V. Loddo, L. Palmisano, *ACS Catal* **2018**, *8*, 11191–11225.

[9] S. Yurdakal, M. Bellardita, I. Pibiri, L. Palmisano, V. Loddo, *Catal Today* **2021**, *380*, 16–24.

[10] M. Bellardita, M. Feilizadeh, R. Fiorenza, S. Scirè, L. Palmisano, V. Loddo, *Photochemical and Photobiological Sciences* **2022**, DOI 10.1007/s43630-022-00284-2.

[11] L. Xiong, J. Tang, *Adv Energy Mater* **2021**, *11*, DOI 10.1002/aenm.202003216.

[12] U. I. Gaya, A. H. Abdullah, *Journal of Photochemistry and Photobiology C: Photochemistry Reviews* **2008**, *9*, 1–12.

[13] L. Palmisano, V. Augugliaro, M. Bellardita, A. Di Paola, E. García López, V. Loddo, G. Marcì, G. Palmisano, S. Yurdakal, *ChemSusChem* **2011**, *4*, 1431–1438.

[14] S. Furukawa, T. Shishido, K. Teramura, T. Tanaka, *ACS Catal* **2012**, *2*, 175–179.

[15] M. Bellardita, S. Yurdakal, B. S. Tek, C. Degirmenci, G. Palmisano, V. Loddo, L. Palmisano, J. Soria, J. Sanz, V. Augugliaro, *J Environ Chem Eng* **2021**, *9*, DOI 10.1016/j.jece.2021.105308.

[16] S. R. Pradhan, V. Nair, D. A. Giannakoudakis, D. Lisovytskiy, J. C. Colmenares, *Molecular Catalysis* **2020**, *486*, DOI 10.1016/j.mcat.2020.110884.

[17] J. Wang, P. Rao, W. An, J. Xu, Y. Men, *Appl Catal B* **2016**, *195*, 141–148.

[18] M. D. Hernández-Alonso, F. Fresno, S. Suárez, J. M. Coronado, *Energy Environ Sci* **2009**, *2*, 1231–1257.

[19] A. Nikokavoura, C. Trapalis, *Appl Surf Sci* **2017**, *391*, 149–174.

[20]   A. Serrà, E. Gómez, J. Michler, L. Philippe, *Chemical Engineering Journal* **2021**, *413*, DOI 10.1016/j.cej.2020.127477.

[21]   A. M. Djaballah, M. Bellardita, L. Palmisano, V. Loddo, M. Umair, C. M. Pecoraro, R. Bagtache, M. Trari, *Molecular Catalysis* **2023**, *546*, 113251.

[22]   X. Xiao, J. Jiang, L. Zhang, *Appl Catal B* **2013**, *142–143*, 487–493.

[23]   S. Higashimoto, N. Suetsugu, M. Azuma, H. Ohue, Y. Sakata, *J Catal* **2010**, *274*, 76–83.

[24]   M. Zhang, Q. Wang, C. Chen, L. Zang, W. Ma, J. Zhao, *Angewandte Chemie International Edition* **2009**, *48*, 6081–6084.

[25]   X. Dai, M. Xie, S. Meng, X. Fu, S. Chen, *Appl Catal B* **2014**, *158–159*, 382–390.

[26]   M. Xie, X. Dai, S. Meng, X. Fu, S. Chen, *Chemical Engineering Journal* **2014**, *245*, 107–116.

[27]   F. Su, S. C. Mathew, G. Lipner, X. Fu, M. Antonietti, S. Blechert, X. Wang, *J Am Chem Soc* **2010**, *132*, 16299–16301.

[28]   M. Bellardita, E. I. García-López, G. Marcì, I. Krivtsov, J. R. García, L. Palmisano, *Appl Catal B* **2018**, *220*, 222–233.

[29]   Y. Song, J. Zhang, X. Dong, H. Li, *Energy Technology* **2021**, *9*, DOI 10.1002/ente.202100033.

[30]   B. Chai, T. Peng, P. Zeng, X. Zhang, X. Liu, *Journal of Physical Chemistry C* **2011**, *115*, 6149–6155.

[31]   C. Liu, Q. Zhang, Z. Zou, *J Mater Sci Technol* **2023**, *139*, 167–188.

[32]   G. Yadav, M. Ahmaruzzaman, *Mater Sci Eng B Solid State Mater Adv Technol* **2023**, *292*, DOI 10.1016/j.mseb.2023.116418.

[33]   Y. Pan, X. Yuan, L. Jiang, H. Yu, J. Zhang, H. Wang, R. Guan, G. Zeng, *Chemical Engineering Journal* **2018**, *354*, 407–431.

[34]   Y. Zhu, L. Wang, Y. Liu, L. Shao, X. Xia, *Appl Catal B* **2019**, *241*, 483–490.

[35]   E. Zhang, Q. Zhu, J. Huang, J. Liu, G. Tan, C. Sun, T. Li, S. Liu, Y. Li, H. Wang, X. Wan, Z. Wen, F. Fan, J. Zhang, K. Ariga, *Appl Catal B* **2021**, *293*, DOI 10.1016/j.apcatb.2021.120213.

[36]   R. Yang, L. Mei, Y. Fan, Q. Zhang, R. Zhu, R. Amal, Z. Yin, Z. Zeng, *Small Methods* **2021**, *5*, DOI 10.1002/smtd.202100887.

[37]   Y. Li, K. Zhang, S. Peng, G. Lu, S. Li, *J Mol Catal A Chem* **2012**, *363–364*, 354–361.

[38]   F. Tian, R. Zhu, K. Song, M. Niu, F. Ouyang, G. Cao, *Mater Res Bull* **2015**, *70*, 645–650.

[39]   C. Tan, G. Zhu, M. Hojamberdiev, K. S. Lokesh, X. Luo, L. Jin, J. Zhou, P. Liu, *J Hazard Mater* **2014**, *278*, 572–583.

[40]   Z. Chen, J. Xu, Z. Ren, Y. He, G. Xiao, *Catal Commun* **2013**, *41*, 83–86.

[41]   L. Su, X. Ye, S. Meng, X. Fu, S. Chen, *Appl Surf Sci* **2016**, *384*, 161–174.

[42]   G. Wang, G. Chen, Y. Yu, X. Zhou, Y. Teng, *RSC Adv* **2013**, *3*, 18579–18586.

[43]   S. Shen, L. Zhao, L. Guo, *Journal of Physics and Chemistry of Solids* **2008**, *69*, 2426–2432.

[44]   N. Ding, Y. Fan, Y. Luo, D. Li, Q. Meng, *APL Mater* **2015**, *3*, DOI 10.1063/1.4930213.

[45]   S. Shen, L. Zhao, L. Guo, *Int J Hydrogen Energy* **2008**, *33*, 4501–4510.

[46]   J. Y. Li, M. Y. Qi, Y. J. Xu, *Chinese Journal of Catalysis* **2022**, *43*, 1084–1091.

[47]   G. Li, X. Nie, Y. Gao, T. An, *Appl Catal B* **2016**, *180*, 726–732.

[48]   J. Zhang, Z. Ma, *RSC Adv* **2017**, *7*, 2163–2171.

[49]   X. Li, J. Li, J. Bai, Y. Dong, L. Li, B. Zhou, *Nanomicro Lett* **2016**, *8*, 221–231.

[50]   G. Wang, G. Chen, Y. Yu, X. Zhou, Y. Teng, *RSC Adv* **2013**, *3*, 18579–18586.

[51]   C. M. Pecoraro, F. Di Franco, M. Bellardita, V. Loddo, M. Santamaria, *Int J Hydrogen Energy* **2023**, DOI 10.1016/j.ijhydene.2023.08.011.

[52]   M. Santamaria, G. Conigliaro, F. Di Franco, B. Megna, F. Di Quarto, *J Electrochem Soc* **2017**, *164*, C113–C120.

[53]   C. L. Tan, M. Y. Qi, Z. R. Tang, Y. J. Xu, *Appl Catal B* **2021**, *298*, DOI 10.1016/j.apcatb.2021.120541.

[54]   M. Bellardita, G. Escolano-Casado, L. Palmisano, L. Mino, *Catal Today* **2022**, DOI 10.1016/j.cattod.2022.12.014.

[55]   G. Palmisano, M. Addamo, V. Augugliaro, T. Caronna, E. García-López, V. Loddo, L. Palmisano, *Chemical Communications* **2006**, 1012–1014.

[56]   S. Yurdakal, G. Palmisano, V. Loddo, O. Alagöz, V. Augugliaro, L. Palmisano, *Green Chemistry* **2009**, *11*, 510–51.

[57]   G. Palmisano, S. Yurdakal, V. Augugliaro, V. Loddo, L. Palmisano, *Adv Synth Catal* **2007**, *349*, 964–970.

[58]   M. Bellardita, H. A. E. Nazer, V. Loddo, F. Parrino, A. M. Venezia, L. Palmisano, *Catal Today* **2017**, *284*, 92–99.

[59]   Z. Chen, J. Xu, Z. Ren, Y. He, G. Xiao, *J Solid State Chem* **2013**, *205*, 134–141.

[60]   V. Augugliaro, T. Caronna, V. Loddo, G. Marcì, G. Palmisano, L. Palmisano, S. Yurdakal, *Chemistry - A European Journal* **2008**, *14*, 4640–4646.

[61]   S. Yurdakal, G. Palmisano, V. Loddo, O. Alagöz, V. Augugliaro, L. Palmisano, *Green Chemistry* **2009**, *11*, 510–51.

[62]   S. Yurdakal, V. Augugliaro, *RSC Adv* **2012**, *2*, 8375–8380.

[63]   M. Bellardita, V. Loddo, G. Palmisano, I. Pibiri, L. Palmisano, V. Augugliaro, *Appl Catal B* **2014**, *144*, 607–613.

[64]   S. Li, L. Meng, W. Tian, L. Li, *Adv Energy Mater* **2022**, *12*, DOI 10.1002/aenm.202200629.